

Effect of Degenerate Particles on Internal Bremsstrahlung of Majorana Dark Matter

Hiroshi Okada^{1*} and Takashi Toma^{2†}

¹*School of Physics, KIAS, Seoul 130-722, Republic of Korea*

²*Laboratoire de Physique Théorique, CNRS - UMR 8627, Université de Paris-Sud 11
F-91405 Orsay Cedex, France*

Abstract

Gamma-rays induced by annihilation or decay of dark matter can be its smoking gun signature. In particular, gamma-rays generated by internal bremsstrahlung of Majorana and real scalar dark matter is promising since it can be a leading emission of sharp gamma-rays. However in the case of Majorana dark matter, its cross section for internal bremsstrahlung cannot be large enough to be observed by future gamma-ray experiments if the observed relic density is assumed to be thermally produced. In this paper, we introduce some degenerate particles with Majorana dark matter, and show they lead enhancement of the cross section. As a result, increase of about one order of magnitude for the cross section is possible without conflict with the observed relic density, and it would be tested by the future gamma-ray experiments such as GAMMA-400 and Cherenkov Telescope Array (CTA). In addition, the constraints of perturbativity, positron observation by the AMS experiment and direct search for dark matter are discussed.

*hokada@kias.re.kr

†takashi.toma@th.u-psud.fr

1 Introduction

The existence of dark matter (DM) is crucial from cosmological observations, however its mass and interaction are not known yet. There are a lot of theoretical DM candidates such as Weakly Interacting Massive Particle (WIMP), axion, gravitino and asymmetric DM. In particular, WIMP is the most promising DM candidate, and experiments are focusing on WIMP detection.

One of the ways to identify nature of DM is indirect detection in which experiments observe such as gamma-rays, neutrinos, positrons and anti-protons coming from the galaxy. Since DM may annihilate or decay into the Standard Model (SM) particles, if observational excess is found over background estimation, it can be a DM signature. Focusing on gamma-rays, known astrophysical sources of gamma-rays induce only smooth spectra, while the DM annihilation or decay may produce a sharp gamma-ray peak. Thus exploring such a line shape spectrum coming from the galaxy is extremely important, and DM models which can induce a strong sharp gamma-ray are fascinating from experimental viewpoint. In fact, the gamma-ray excesses from the galactic center have been reported by several papers [1, 2] and [3–5]. The former implies the DM mass to be 130-135 GeV with its partial annihilation cross section $\sigma v \sim 10^{-27} \text{ cm}^3/\text{s}$ into gamma-rays. However this signal has disappeared after the dedicated analysis by the Fermi Collaboration [6]. The latter has found rather mild excess around 10 GeV which could be caused by 30-60 GeV of the DM mass with a specific annihilation mode such as a pair of bottoms or taus. The partial cross section should be $\sigma v \sim 10^{-26} \text{ cm}^3/\text{s}$ that is very close to the cross section for thermal production of the observed relic density.

Representative processes inducing sharp gamma-rays are two-body annihilations such as $\chi\chi \rightarrow \gamma\gamma$ and $\chi\chi \rightarrow \gamma Z$. Since the energy of the photon is kinematically determined as $E_\gamma = m_\chi$ for $\gamma\gamma$ channel and $E_\gamma = m_\chi (1 - m_Z^2/(4m_\chi^2))$ for γZ channel, gamma-rays become monochromatic. However, the cross sections for these processes are typically expected to be small because of loop suppression. Another process of sharp gamma-rays is internal bremsstrahlung $\chi\chi \rightarrow f\bar{f}\gamma$ [7–13].¹ When the two-body process $\chi\chi \rightarrow f\bar{f}$ is chirally-suppressed, the internal bremsstrahlung process becomes important for the gamma-ray source of DM. The cross section for this process becomes larger than monochromatic gamma-ray processes since this is three-body process at tree level. The gamma-ray spectrum of internal bremsstrahlung can be very sharp if mass of the mediate particle is not far from the DM mass. This is because fermion and anti-fermion with soft energy is produced in the final state and the most energy of the initial state is taken away by the other two particles. As a result, the energy of photon is almost fixed to half of the total energy of the initial state $2m_\chi$. In particular for real scalar DM, stronger sharp gamma-rays can be induced than the Majorana DM case due to d-wave suppression of the two-body process $\chi\chi \rightarrow f\bar{f}$ [16–19]. In the case of Majorana DM, it

¹There is also a model which produces a characteristic box-type gamma-ray spectrum mediated by a light axion-like scalar [14, 15].

is known that the cross section for internal bremsstrahlung $\chi\chi \rightarrow f\bar{f}\gamma$ cannot be large enough to be detected in near future if thermal production of DM is concerned [12]. This is because suppression for $\chi\chi \rightarrow f\bar{f}$ is p-wave and once the interaction strength is fixed in order to obtain the observed relic density of DM, the cross section for internal bremsstrahlung is also determined. It has been claimed that the gamma-ray spectrum of internal bremsstrahlung can reproduce nicely the 130-135 GeV line mentioned above, however this is not compatible with thermal relic density of DM [1]. One should note that the internal bremsstrahlung process is also constrained by AMS positron observation since a pair of high energy electron and positron is also produced [20, 21].

In this paper, we consider enhancement of the internal bremsstrahlung process for Majorana DM due to increase of DM effective degrees of freedom taking into account degenerate particles with DM. Assuming that the degenerate particles weakly interact with the SM particles, the effective annihilation cross section for relic density would be smaller than the DM self-annihilation cross section. Thus the interaction of DM should be larger in order to satisfy the observed DM relic density. As a result, it is expected that the cross section for internal bremsstrahlung is also increased. Moreover we will consider the constraints from perturbativity, positron observation by the AMS experiment and direct detection experiments. A similar work has been done for a Higgsino- or Wino-like neutralino DM in a supersymmetric model [22]. In this reference, the authors have considered co-annihilations with sleptons. Because of increase of DM couplings for the correct relic density due to weak co-annihilations, annihilation rates into neutrinos and anti-protons have been enhanced as indirect detection signals of DM. Our work in this paper is an application to internal bremsstrahlung in a simplified Majorana DM model.

This paper is organized as follows. In the next section, we quantitatively review the standard internal bremsstrahlung of a single Majorana DM, and explicitly show the cross section for the process cannot be large enough to be detected by future gamma-ray experiments. In Section 3, we introduce several degenerate particles with DM and show enhancement of the cross section is derived due to the degenerate particles. Our conclusions are given in Section 4.

2 Standard Internal bremsstrahlung

2.1 Interactions and cross sections

We consider the leptonic Yukawa interaction

$$\mathcal{L} = y\varphi\bar{\chi}P_R\ell + \text{H.c.}, \quad (1)$$

where the Yukawa coupling y is assumed to be real for simplicity, χ is a singlet Majorana DM in the SM gauge group, φ is an electromagnetically charged scalar mediator with hypercharge $Y_\varphi = 1$ and ℓ is a right-handed charged lepton. Although DM can couple to three generations of the charged leptons in general, we consider an interaction with only

one generation for simplicity. DM is regarded to be stabilized by a \mathbb{Z}_2 symmetry. In our case, \mathbb{Z}_2 assignment should be odd for DM χ and the mediator φ and even for the charged lepton ℓ .

The thermal relic density of DM is determined by the annihilation cross section into a pair of leptons through the Yukawa coupling, and should satisfy the observed one $\Omega h^2 \approx 0.120$ [23]. When the DM mass is much heavier than the charged lepton mass $m_\ell/m_\chi \ll 1$, the annihilation cross section into $\ell\bar{\ell}$ is calculated as

$$\sigma v_{\ell\bar{\ell}} = \frac{y^4}{48\pi m_\chi^2} \frac{1 + \mu^2}{(1 + \mu)^4} v^2, \quad (2)$$

where $\mu = m_\varphi^2/m_\chi^2$ is the mass ratio between DM and the mediator, and v is the relative velocity of DM. There is no s-wave due to chiral suppression. The required strength of the Yukawa coupling for the several fixed mass ratios m_φ/m_χ is shown in the left panel in Fig. 1. As one can see from the figure, $\mathcal{O}(1)$ Yukawa coupling is needed for the measured relic density. When the mass ratio is $m_\varphi/m_\chi = 1.01$, the required Yukawa coupling becomes rather small since the co-annihilation with the mediator is strong. In this case, the DM mass being less than 170 GeV gives too small relic density and cannot satisfy the measured relic density. There is a small dip around $m_\chi \approx 40$ GeV for $m_\varphi/m_\chi = 1.1$. This is because DM and the mediator φ are 10% degenerate, and the effective annihilation cross section of DM becomes large due to the φ self-annihilation channel: $\varphi^\dagger\varphi \rightarrow f\bar{f}$ mediated by the s-channel Z boson where f is a SM fermion. The region of the DM mass more than a few TeV tends to be ruled out by perturbativity of the Yukawa coupling.

As one can see from Eq. (2), the cross section is suppressed by the relative velocity squared (p-wave) due to the helicity suppression. Because of that, this channel is extremely suppressed in current times since the averaged DM relative velocity is roughly $v \sim 10^{-3}$. As a result, three-body process $\chi\chi \rightarrow \ell\bar{\ell}\gamma$ becomes important for indirect detection of DM [7–13]. There are three diagrams contributing to the process. The total amplitude is separated to Final State Radiation (FSR) and Virtual Internal Bremsstrahlung (VIB) parts in a gauge invariant way [9, 10]. Among them, the differential cross section of the FSR contribution is model-independently given by

$$\frac{d\sigma v_{\ell\bar{\ell}\gamma}^{\text{FSR}}}{dx} = \sigma v_{\ell\bar{\ell}} \frac{\alpha_{\text{em}}}{\pi} \frac{(1-x)^2 + 1}{x} \log\left(\frac{4m_\chi^2(1-x)}{m_\ell^2}\right), \quad (3)$$

where $x = E_\gamma/m_\chi$. Since this cross section is proportional to the chirally-suppressed two-body cross section $\sigma v_{\ell\bar{\ell}}$, the FSR contribution to the gamma-ray source is negligible. Therefore the other VIB contribution becomes dominant.² This process may induce sharp gamma-ray spectrum when the φ mass is not far from the DM mass ($\mu \lesssim 2$). In the limit

²The interference term with the amplitude for FSR is also negligible in the region of $E_\gamma \sim m_\chi$.

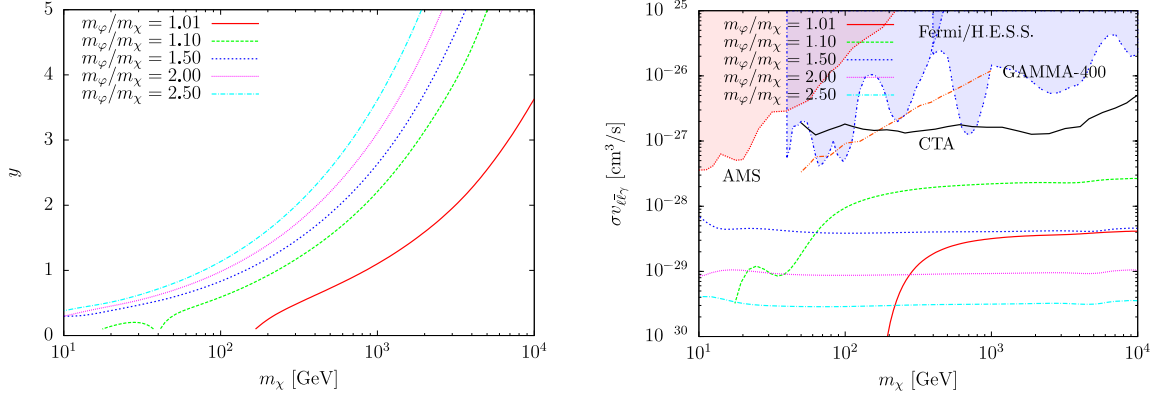


Figure 1: Contours satisfying the measured DM relic density on (m_χ, y) plane (left panel). Comparison of the cross section for internal bremsstrahlung with gamma-ray experiments and the AMS positron observation (right panel).

of $m_\ell/m_\chi \rightarrow 0$, the cross section for internal bremsstrahlung $\chi\chi \rightarrow \ell\bar{\ell}\gamma$ is calculated as [9]

$$\sigma v_{\ell\bar{\ell}\gamma} = \frac{y^4 \alpha_{\text{em}}}{64\pi^2 m_\chi^2} \left[(\mu + 1) \left\{ \frac{\pi^2}{6} - \log^2 \left(\frac{\mu + 1}{2\mu} \right) - 2\text{Li}_2 \left(\frac{\mu + 1}{2\mu} \right) \right\} + \frac{4\mu + 3}{\mu + 1} + \frac{(4\mu + 1)(\mu - 1)}{2\mu} \log \left(\frac{\mu - 1}{\mu + 1} \right) \right]. \quad (4)$$

There are also the loop-induced channels $\chi\chi \rightarrow \gamma\gamma$ and $\chi\chi \rightarrow \gamma Z$ as the other gamma-ray sources. In this model, the annihilation cross section for $\chi\chi \rightarrow \gamma\gamma$ is calculated as [19]

$$\sigma v_{\gamma\gamma} = \frac{y^4 \alpha_{\text{em}}^2}{256\pi^3 m_\chi^2} \left| \text{Li}_2 \left(\frac{1}{\mu} \right) - \text{Li}_2 \left(-\frac{1}{\mu} \right) \right|^2. \quad (5)$$

This cross section is typically smaller than the cross section for internal bremsstrahlung at $\mu \sim 1$ due to the loop suppression as have discussed in ref. [19], and the cross section for $\chi\chi \rightarrow \gamma Z$ is also small. If DM χ has the other interactions with the SM particles and annihilates as $\chi\chi \rightarrow b\bar{b}, W^+W^-, ZZ$, continuous broad gamma-rays are produced and it should be included in total gamma-ray sources from DM. In particular, if the mediator φ has a $SU(3)_c$ charge, anti-protons are produced due to gluon internal bremsstrahlung $\chi\chi \rightarrow q\bar{q}g$ through the interaction $y\varphi\bar{\chi}q$ which is obtained by replacing the charged lepton ℓ with a quark q [24]. This gluon internal bremsstrahlung would give a stronger constraint than photon internal bremsstrahlung. However in this simplified model, such annihilations do not occur since the $SU(3)_c$ singlet mediator φ is concerned.

The cross section for internal bremsstrahlung is numerically calculated by using the Yukawa coupling which satisfies the observed relic density as shown in the right panel in Fig. 1. In the region of $m_\chi \lesssim 300$ GeV for $m_\varphi/m_\chi = 1.01$, since the co-annihilation and self-annihilation of φ are dominant, the Yukawa coupling needed for the observed relic density becomes small. Therefore, the cross section for internal bremsstrahlung is

also small. For $m_\varphi/m_\chi \approx 1.10$, the cross section can be maximal, and for larger mass ratio, although the required Yukawa coupling for the observed relic density can be sizable, the cross section for internal bremsstrahlung remains small since it decreases rapidly as $\sigma v_{\ell\bar{\ell}\gamma} \propto \mu^{-4}$ for $\mu \gg 1$.

2.2 Gamma-ray bounds, prospects and AMS positron observation

In order to set an upper bound for the cross section generating sharp gamma-rays, the cross section is translated to gamma-ray flux and specific target region of interest for observation is taken as followed by ref. [12]. The Fermi/H.E.S.S. limit has been obtained by assuming an Einasto DM profile with appropriate parameter setting in ref. [12]. The Fermi and H.E.S.S. data were taken from search region 3 Pass 7 SOURCE sample in ref [2] and the central Galactic halo (CGH) region in ref. [25] respectively. As shown in the right panel of Fig. 1, the blue region is excluded by Fermi-LAT and H.E.S.S. at 95% Confidence Level (CL) [12], and the prospected sensitivities of the future gamma-ray experiments GAMMA-400 and Cherenkov Telescope Array (CTA) are described by the brown and black lines [26, 27]. As one can see, the maximal cross section for sharp gamma-rays in the case of standard internal bremsstrahlung is about $\sigma v_{\ell\bar{\ell}\gamma} \approx 2 \times 10^{-28} \text{ cm}^3/\text{s}$ which is about one order of magnitude below the GAMMA-400 and CTA prospects.

Since high energy charged leptons are also produced by internal bremsstrahlung, the cross section for $\chi\chi \rightarrow \ell\bar{\ell}\gamma$ is constrained by the AMS positron observation [20]. The upper bound of the cross section for internal bremsstrahlung $\chi\chi \rightarrow e^+e^-\gamma$ has been studied by in ref. [21] where an Einasto DM profile is assumed. This upper bound is shown as the red region in the right panel of Fig. 1. Note that even if $\ell = \mu, \tau$, high energy electrons and positrons are emitted from the μ, τ decays. However since their energy is softer than that of direct produced e^+e^- , the constraint for $e^+e^-\gamma$ would be strongest and regarded as conservative upper bound for $\chi\chi \rightarrow \ell\bar{\ell}\gamma$.

As we have discussed here, the cross section for the standard internal bremsstrahlung of Majorana dark matter cannot reach the prospected sensitivity of the future gamma-ray experiments. Hence we move on to our scenario to obtain a larger cross section for internal bremsstrahlung in the next section.

3 Internal Bremsstrahlung with Degenerate Particles

3.1 Interactions and cross sections

Now we consider k degenerate Majorana fermions with DM. The Yukawa interaction is extended by

$$\mathcal{L} = \sum_{i=1}^k y_i \varphi \bar{\chi}_i P_R \ell + \text{H.c.}, \quad (6)$$

where χ_1 is the lightest and regarded as DM with the mass $m_1 \equiv m_\chi$, χ_i ($i \neq 1$) is assumed to be degenerate with DM whose mass is denoted as m_i ($i \neq 1$). In general, we can choose the diagonal base for the mass matrix of χ_i . When DM is degenerate with these particles, co-annihilation effect has to be taken into account to evaluate thermal relic density of DM. Following ref. [28], the effective annihilation cross section is given by

$$\sigma_{\text{eff}} v = \sum_{i=1}^k \sum_{j=1}^k \frac{g_i g_j}{g_{\text{eff}}^2} \sigma_{ij} v (1 + \Delta_i)^{3/2} (1 + \Delta_j)^{3/2} e^{-(\Delta_i + \Delta_j)x}, \quad (7)$$

where g_{eff} is the effective degrees of freedom

$$g_{\text{eff}} = \sum_{i=1}^k g_i (1 + \Delta_i)^{3/2} e^{-\Delta_i x}, \quad (8)$$

and $\Delta_i \equiv (m_i - m_1)/m_1$ is the mass difference between DM and the other degenerate particles, $g_i = 2$ is the degrees of freedom for each Majorana particle χ_i , $x = m_1/T$ and $\sigma_{ij} v$ is (co-)annihilation cross section between i and j . If a lot of degenerate particles exist, the effective degrees of freedom g_{eff} increases. In addition, the Yukawa coupling y_i ($i \neq 1$) is larger than y_1 , its effective annihilation cross section $\sigma_{\text{eff}} v$ also becomes large and the relic density of the DM is much reduced. On the other hand, if the Yukawa coupling y_i ($i \neq 1$) is smaller than y_1 , the effective annihilation cross section becomes smaller than the standard cross section of DM for non-degenerate case ($k = 1$). Thus to compensate the lack of the cross section, a larger coupling of DM y_1 is required to satisfy the observed relic density. We consider such a small Yukawa coupling y_i ($i \neq 1$) for the degenerate fermions to increase the strength of the DM Yukawa coupling y_1 . The cross section for internal bremsstrahlung is given by the same formula with Eq. (4) and replacing $y \rightarrow y_1$.

We give some numerical results for effect of the DM Yukawa coupling due to the degenerate Majorana fermions. The effective cross section has been calculated by micrOMEGAs [29]. The cross section for internal bremsstrahlung obtained in the degenerate scenario in terms of the mass ratio between DM and the mediator (m_φ/m_1) is shown in Fig. 2, where the DM mass m_1 is fixed to be 300 GeV and the mass ratio between the degenerate particles and DM m_i/m_1 is fixed to 1.01 as an example. We assumed that

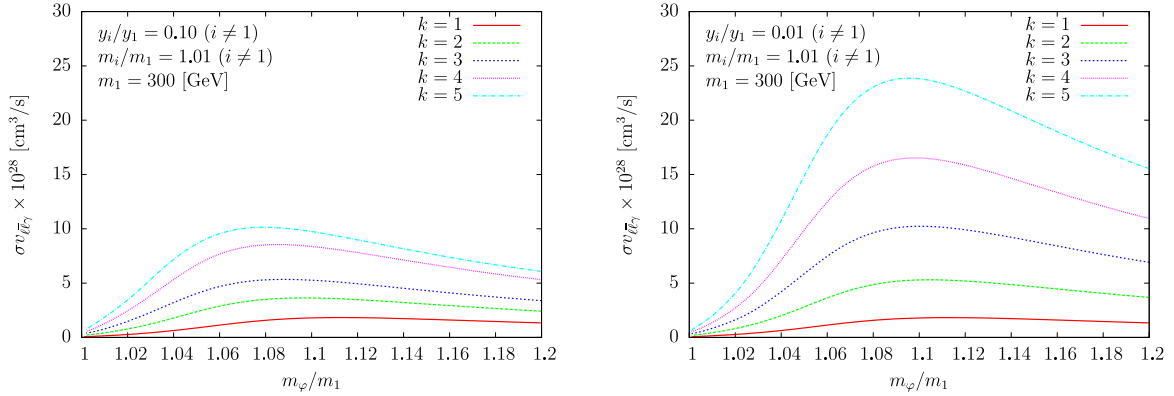


Figure 2: m_φ/m_1 dependence of the cross section for internal bremsstrahlung. The strength of the Yukawa coupling y_i ($i \neq 1$) compared to y_1 is taken as $y_i/y_1 = 0.10$ (left panel) and $y_i/y_1 = 0.01$ (right panel).

all the degenerate fermions have same masses for simplicity. The strength of the Yukawa coupling y_i/y_1 ($i \neq 1$) is fixed to be 0.10 in the left panel, and 0.01 in the right panel. The figure shows that larger enhancement of the cross section can be obtained in the case of a smaller y_i/y_1 and a larger number of degenerate particles as we expected. One also finds that a mild peak exists at a value of m_φ/m_1 depending on the parameters. The position of the peak is in the range of $1.06 \lesssim m_\varphi/m_1 \lesssim 1.12$.

The dependence on the mass degeneracy m_i/m_1 of the DM Yukawa coupling required for thermal DM production is shown in Fig. 3 where the mass ratio m_φ/m_1 and the strength of the Yukawa coupling y_i are fixed as shown in the figure. The mass ratio m_φ/m_1 should be $\mu \lesssim 2$ to get a sharp gamma-ray peak of internal bremsstrahlung. As one can see from the figure, when the number of the particles increases and they are strongly degenerate, the required strength of the DM Yukawa coupling for the observed relic density is enhanced. According to the figure, it is possible to obtain one order of magnitude increase of $(y_1/y)^4$. We should note that for $m_\varphi/m_1 = 1.01$, large enhancement of the Yukawa coupling occurs, however the cross section for internal bremsstrahlung cannot be so large since the absolute value of the Yukawa coupling is small. Although the DM mass must be fixed to calculate thermal relic density, there is almost no dependence on the DM mass. The reason is that we take the ratio of the cross sections Eq. (2) and $\sigma_{11}v$ in Eq. (7) to derive the ratio of the Yukawa coupling $(y_1/y)^4$, and the ratio of the cross sections is dimensionless.

3.2 Gamma-rays and the other constraints

The comparison with the Fermi/H.E.S.S. bound and the future gamma-ray experiments GAMMA-400 and CTA is shown in Fig. 4 where the mass ratio m_φ/m_1 and the Yukawa coupling of the degenerate fermions are fixed as same as Fig. 3. In particular,

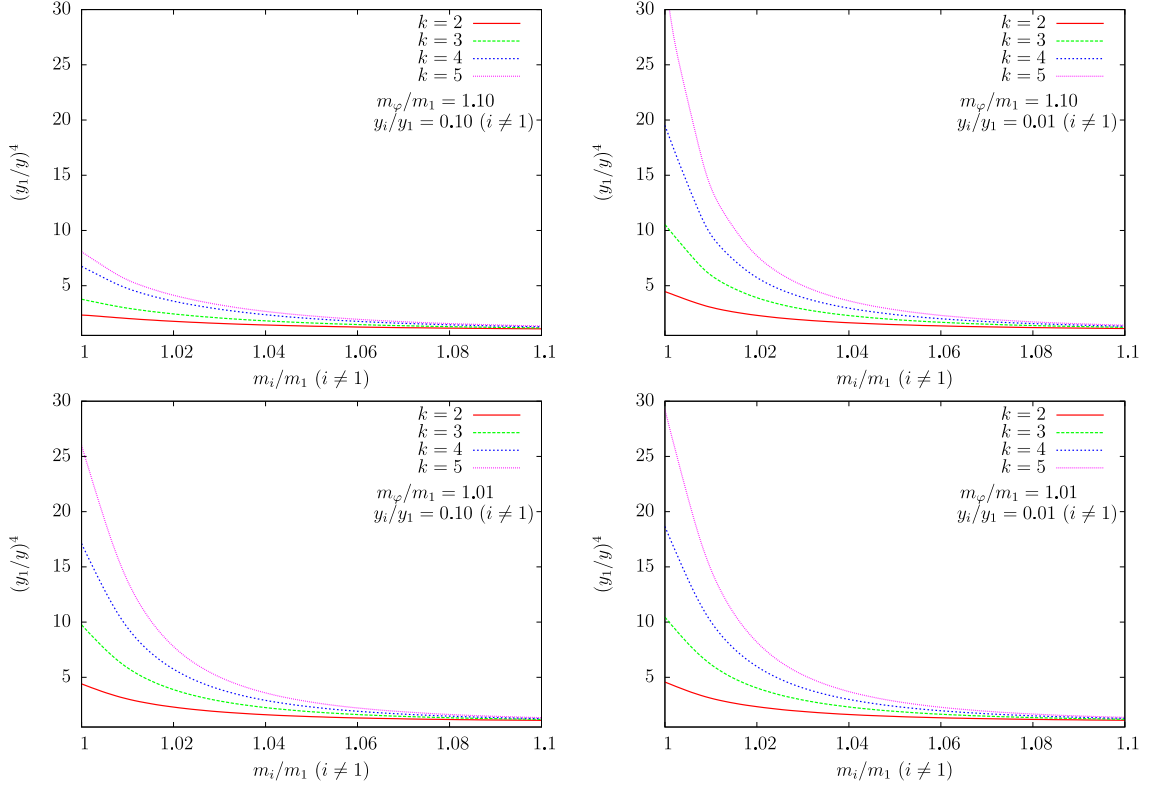


Figure 3: Mass degeneracy dependence of the Yukawa coupling required for thermal relic density where y in the y-axis is the Yukawa coupling for non-degenerate case, and all the degenerate fermion masses m_i ($i \neq 1$) are assumed to be same.

one can see that for $m_\varphi/m_1 = 1.10$ and $y_i/y_1 = 0.01$ (upper right panel), the cross section for internal bremsstrahlung is largely enhanced and testable by GAMMA-400 and CTA [26, 27]. For $m_\varphi/m_1 = 1.01$, the cross section is rather smaller than the case for $m_\varphi/m_1 = 1.10$ due to the strong co-annihilation with φ .

Some other constraints are also shown in Fig. 4. The conservative perturbativity bound $y_1 \leq \sqrt{4\pi}$ is taken into account and the excluded region is shown in the figure as grey color. This bound depends on the mass ratio m_φ/m_1 . The red region is excluded by the AMS positron observation as discussed above. In addition, we should note that when DM and the mediator φ are extremely degenerate as less than 1%, direct searches for DM may affect to the analysis even if a leptophilic DM is concerned because an interaction between DM and quarks is derived at one-loop level. For Majorana DM, only anapole interaction a which is given by

$$\mathcal{L}_{\text{eff}} = a \bar{\chi} \gamma^\mu \gamma_5 \chi \partial^\nu F_{\mu\nu}, \quad (9)$$

is relevant for direct detection of DM where $F_{\mu\nu}$ is the electromagnetic field strength.³ The concrete expression of the anapole moment and the related loop function have been

³When a Majorana DM and an excited DM χ_i ($i \neq 1$) are degenerate as in our framework, transition

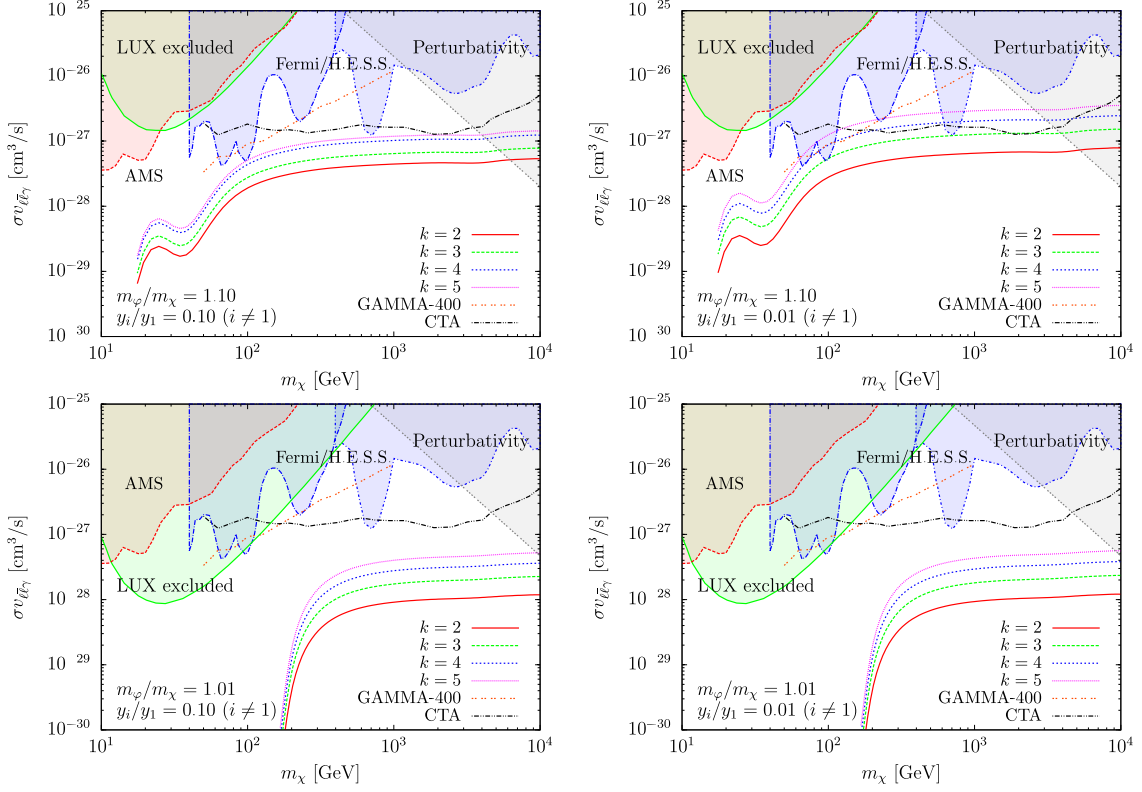


Figure 4: Comparison of the cross section for internal bremsstrahlung with gamma-ray experiments where m_φ/m_1 and y_i/y_1 are fixed as in each figure, and $m_i/m_1 = 1.01$. The grey, green and red regions are excluded by perturbativity of the Yukawa coupling y_1 , the LUX experiment and the AMS positron observation respectively.

obtained in ref. [13]. The elastic cross section with nuclei derived from the anapole moment is suppressed by the DM velocity squared. However according to ref. [13], when DM χ_1 and the charged mediator φ are extremely degenerate as less than a few %, direct searches for DM would give a constraint on the cross section for internal bremsstrahlung due to the existence of a pole of the anapole moment at $m_\varphi/m_1 = 1$. Enhancement of the anapole moment is especially large when DM interacts with electron, not but muon and tau since the anapole moment is proportional to $\log(m_\ell^2/m_\chi^2)$ for $|q|^2 \ll m_\ell^2$ where $|q| \lesssim m_\mu$ is the transfer momentum of photon. For $|q|^2 \gg m_\ell^2$, this factor is replaced by $\log(|q|^2/m_\chi^2)$. Thus the strongest constraint is obtained for electron. The green region in Fig. 4 is excluded by the LUX experiment where the coupling with electron is assumed. In particular, the mass degeneracy between DM and the mediator is $m_\varphi/m_1 = 1.01$, a lower DM mass region expected to be tested by the future gamma-ray experiments is excluded.

DM and the charged scalar masses may be constrained by the LHC as well since a dipole interactions among them may be obtained if CP phase exists in the Yukawa coupling [30]. However in this paper, since we assumed real Yukawa couplings, the transition dipole moment does not exist.

pair of the charged scalar φ can be produced via the Drell-Yan process. The bound for slepton search via the channel $q\bar{q} \rightarrow \gamma/Z^* \rightarrow \tilde{\ell}\tilde{\ell}^\dagger \rightarrow \ell\bar{\ell} + \cancel{E}$ would be applied for our case as good approximation because the charged scalar φ can be regarded as a kind of slepton. The ATLAS and CMS Collaborations have analyzed 20.3 fb^{-1} and 19.5 fb^{-1} of the LHC data at $\sqrt{s} = 8 \text{ TeV}$ respectively, and the constraints for the DM and slepton masses have been derived [31, 32]. However since we are interested in degenerate mass region between DM and the charged scalar, the constraint of the LHC is relaxed and there is no substantial constraint for $m_\varphi/m_1 \lesssim 1.2$. Note that if the charged lepton ℓ in our framework is replaced to a quark, much stronger constraint is imposed by the LHC.

4 Conclusions and Discussions

Identifying DM is one of the primary issues in (astro-)particle physics. Looking for line like gamma-rays coming from the galaxy is important for DM searches since some DM candidates can generate sharp gamma-rays which are not expected to be induced by astrophysical sources. In particular, internal bremsstrahlung of DM shows an interesting sharp gamma-ray spectrum. We have considered internal bremsstrahlung for leptophilic Majorana DM with degenerate particles. When the degenerate particles have the Yukawa coupling which is smaller than that for DM, we need a larger Yukawa coupling for DM to satisfy the measured relic density. As a result, the cross section for internal bremsstrahlung has been enhanced. More than one order of magnitude of increase has been achieved for some parameter sets, and it can be testable by the future gamma-ray experiments. We have also considered the constraints from perturbativity of the DM Yukawa coupling, the AMS positron observation and direct search for DM via anapole moment. While the elastic cross section with nucleon derived from anapole moment is suppressed by the DM velocity, a parameter space has been excluded because of huge enhancement of the anapole moment at $m_\varphi/m_1 \approx 1$.

Finally we briefly comment on the other aspects. Small mass difference as we have considered would be induced by introducing an extra $U(1)$ or a flavor symmetry. For example, one can construct a model that one Dirac fermion DM with a charge of the extra $U(1)$ symmetry is split to two degenerate Majorana fermions after symmetry breaking. Furthermore, the leptophilic DM we have considered in this paper can be identified as the TeV scale right-handed neutrino. Such a TeV or electroweak scale right-handed neutrino is included in some models with radiative neutrino masses. Thus our framework discussed in this paper naturally works in these models.

Acknowledgments

T. T. acknowledges support from the European ITN project (FP7-PEOPLE-2011-ITN, PITN-GA-2011-289442-INVISIBLES) and P2IO Excellence Laboratory (Labex).

References

- [1] T. Bringmann, X. Huang, A. Ibarra, S. Vogl and C. Weniger, JCAP **1207**, 054 (2012) [[arXiv:1203.1312](#) [hep-ph]].
- [2] C. Weniger, JCAP **1208**, 007 (2012) [[arXiv:1204.2797](#) [hep-ph]].
- [3] D. Hooper and T. Linden, Phys. Rev. D **84**, 123005 (2011) [[arXiv:1110.0006](#) [astro-ph.HE]].
- [4] K. N. Abazajian, N. Canac, S. Horiuchi and M. Kaplinghat, Phys. Rev. D **90**, 023526 (2014) [[arXiv:1402.4090](#) [astro-ph.HE]].
- [5] E. Carlson, D. Hooper and T. Linden, [arXiv:1409.1572](#) [astro-ph.HE].
- [6] M. Ackermann *et al.* [Fermi-LAT Collaboration], Phys. Rev. D **88**, 082002 (2013) [[arXiv:1305.5597](#) [astro-ph.HE]].
- [7] L. Bergstrom, Phys. Lett. B **225**, 372 (1989).
- [8] R. Flores, K. A. Olive and S. Rudaz, Phys. Lett. B **232**, 377 (1989).
- [9] T. Bringmann, L. Bergstrom and J. Edsjo, JHEP **0801**, 049 (2008) [[arXiv:0710.3169](#) [hep-ph]].
- [10] P. Ciafaloni, M. Cirelli, D. Comelli, A. De Simone, A. Riotto and A. Urbano, JCAP **1106**, 018 (2011) [[arXiv:1104.2996](#) [hep-ph]].
- [11] V. Barger, W. Y. Keung and D. Marfatia, Phys. Lett. B **707**, 385 (2012) [[arXiv:1111.4523](#) [hep-ph]].
- [12] M. Garny, A. Ibarra, M. Pato and S. Vogl, JCAP **1312**, 046 (2013) [[arXiv:1306.6342](#) [hep-ph]].
- [13] J. Kopp, L. Michaels and J. Smirnov, JCAP **1404**, 022 (2014) [[arXiv:1401.6457](#) [hep-ph]].
- [14] A. Ibarra, S. Lopez Gehler and M. Pato, JCAP **1207**, 043 (2012) [[arXiv:1205.0007](#) [hep-ph]].
- [15] A. Ibarra, H. M. Lee, S. López Gehler, W. I. Park and M. Pato, JCAP **1305**, 016 (2013) [[arXiv:1303.6632](#) [hep-ph]].
- [16] T. Toma, Phys. Rev. Lett. **111**, 091301 (2013) [[arXiv:1307.6181](#) [hep-ph]].
- [17] F. Giacchino, L. Lopez-Honorez and M. H. G. Tytgat, JCAP **1310**, 025 (2013) [[arXiv:1307.6480](#) [hep-ph]].
- [18] A. Ibarra, T. Toma, M. Totzauer and S. Wild, Phys. Rev. D **90**, 043526 (2014) [[arXiv:1405.6917](#) [hep-ph]].
- [19] F. Giacchino, L. Lopez-Honorez and M. H. G. Tytgat, JCAP **1408**, 046 (2014) [[arXiv:1405.6921](#) [hep-ph]].
- [20] M. Aguilar *et al.* [AMS Collaboration], Phys. Rev. Lett. **110**, 141102 (2013).

- [21] L. Bergstrom, T. Bringmann, I. Cholis, D. Hooper and C. Weniger, Phys. Rev. Lett. **111**, 171101 (2013) [[arXiv:1306.3983](#) [astro-ph.HE]].
- [22] S. Profumo and A. Provenza, JCAP **0612**, 019 (2006) [[hep-ph/0609290](#)].
- [23] P. A. R. Ade *et al.* [Planck Collaboration], Astron. Astrophys. **571**, A16 (2014) [[arXiv:1303.5076](#) [astro-ph.CO]].
- [24] M. Asano, T. Bringmann and C. Weniger, Phys. Lett. B **709**, 128 (2012) [[arXiv:1112.5158](#) [hep-ph]].
- [25] A. Abramowski *et al.* [HESS Collaboration], Phys. Rev. Lett. **110**, 041301 (2013) [[arXiv:1301.1173](#) [astro-ph.HE]].
- [26] A. M. Galper, O. Adriani, R. L. Aptekar, I. V. Arkhangelskaja, A. I. Arkhangelskiy, M. Boezio, V. Bonvicini and K. A. Boyarchuk *et al.*, Adv. Space Res. **51**, 297 (2013) [[arXiv:1201.2490](#) [astro-ph.IM]].
- [27] K. Bernlöhr, A. Barnacka, Y. Becherini, O. Blanch Bigas, E. Carmona, P. Colin, G. Decerprit and F. Di Pierro *et al.*, Astropart. Phys. **43**, 171 (2013) [[arXiv:1210.3503](#) [astro-ph.IM]].
- [28] K. Griest and D. Seckel, Phys. Rev. D **43**, 3191 (1991).
- [29] G. Belanger, F. Boudjema, A. Pukhov and A. Semenov, Comput. Phys. Commun. **185**, 960 (2014) [[arXiv:1305.0237](#) [hep-ph]].
- [30] D. Schmidt, T. Schwetz and T. Toma, Phys. Rev. D **85**, 073009 (2012) [[arXiv:1201.0906](#) [hep-ph]].
- [31] G. Aad *et al.* [ATLAS Collaboration], JHEP **1405**, 071 (2014) [[arXiv:1403.5294](#) [hep-ex]].
- [32] V. Khachatryan *et al.* [CMS Collaboration], Eur. Phys. J. C **74**, no. 9, 3036 (2014) [[arXiv:1405.7570](#) [hep-ex]].